PROTEINS: Structure, Function, and Bioinformatics 64:355–362 (2006)

Interaction of (−)-Epigallocatechin-3-Gallate With Human Serum Albumin: Fluorescence, Fourier Transform Infrared, Circular Dichroism, and Docking Studies

Tushar Kanti Maiti, Kalyan Sundar Ghosh, and Swagata Dasgupta*
Department of Chemistry, Indian Institute of Technology, Kharagpur, India

ABSTRACT **(−)-Epigallocatechin-3-gallate (EGCG), the major constituent of green tea has been reported to prevent many diseases by virtue of its antioxidant properties. The binding of EGCG with human serum albumin (HSA) has been investigated for the first time by using fluorescence, circular dichroism (CD), Fourier transform infrared (FTIR) spectroscopy, and protein-ligand docking. We observed a quenching of fluorescence of HSA in the presence of EGCG. The binding parameters were determined by a Scatchard plot and the results were found to be consistent with those obtained from a modified Stern-Volmer equation. From the thermodynamic parameters calculated according to the van't Hoff equation, the enthalpy change $\Delta H°$ and entropy change $\Delta S°$ were found to be −22.59 and 16.23 J/mol K, respectively. These values suggest that apart from an initial hydrophobic association, the complex is held together by van der Waals interactions and hydrogen bonding. Data obtained by fluorescence spectroscopy, CD, and FTIR experiments along with the docking studies suggest that EGCG binds to residues located in subdomains IIa and IIIa of HSA. Specific interactions are observed with residues Trp 214, Arg 218, Gln 221, Asn 295 and Asp 451. We have also looked at changes in the accessible surface area of the interacting residues on binding EGCG for a better understanding of the interaction. Proteins 2006;64:355–362.**

Key words: (−)-epigallocatechin-3-gallate; human serum albumin; fluorescence quenching; FTIR; circular dichroism; FlexX single molecule docking; accessible surface area

INTRODUCTION

Green tea has become a subject of growing interest because of its multifarious properties. The leaves of green tea contain a special class of bioflavonoids, catechin polyphenols, with antioxidant properties.[1] The polyphenols increase the level of antioxidants in the body that neutralize free radicals before they cause cell damage.[2] Green tea has also shown the presence of active anticancer constituents[3–6] and studies relating angiogenesis and green tea catechins have focused on their ability to inhibit the process of growth of new blood vessels.[7] They are thought to block the attachment of carcinogens and bacteria to cells, and support healthy liver function.[8] Thus, plant phenolic compounds are multifunctional antioxidants that can act as metal chelators,[9,10] singlet oxygen quenchers, or reducing agents (free-radical terminators).[1,2] The catechins in green tea with antioxidant activity have been characterized as (−)-epicatechin (EC), (−)-epigallocatechin (EGC), (−)-epicatechin gallate (ECG), and (−)-epigallocatechin-3-gallate (EGCG). Among these, EGCG is the major (comprising ~50% of the total catechins present) and most potent constituent of green tea (Fig. 1).[3,4]

HSA, the most abundant protein in the serum, is the most important drug carrier protein.[11] Apart from an important role in maintaining the colloidal osmotic pressure in blood, it is responsible for the transport and distribution of many exogenous and endogenous molecules and metabolites such as nutrients, hormones, fatty acids, and many diverse drugs.[12] It also binds and transports many drug molecules through the blood stream, which are poorly soluble in water. HSA is a globular protein consisting of 585 amino acid residues and is considered to have three specific domains, I, II, and III, each of which consist of two subdomains, a and b possessing common structural motifs.[13,14] Crystal structure analysis has revealed that HSA has binding sites of compounds within specialized cavities in subdomains IIa and IIIa (Fig. 2), which correspond to site I and site II, respectively. The sole tryptophan residue (Trp 214) of HSA is in subdomain IIa.

A considerable amount of research has been directed toward the activity of polyphenols as antioxidants and radical scavengers, as well as their antimutagenic and anticarcinogenic properties. A number of biochemical and molecular biological investigations have revealed that proteins are frequently the "targets" for therapeutically active flavonoids and isoflavonoids of both natural and synthetic origin.[15] However, to date, little is known about

Abbreviations: HSA, human serum albumin; EGCG, (−)-epigallocatechin-3-gallate; FTIR, Fourier transform infrared; CD, circular dichroism; PDB, Protein Data Bank; ASA, accessible surface area.

Grant sponsor: Department of Science and Technology (DST); Grant sponsor: Ministry of Human Resource Development (MHRD), Government of India.

*Correspondence to: Swagata Dasgupta, Department of Chemistry, Indian Institute of Technology, Kharagpur 721302, India. E-mail: swagata@chem.iitkgp.ernet.in

Received 6 September 2005; Revised 9 January 2006; Accepted 24 February 2006

Published online 16 May 2006 in Wiley InterScience (www.interscience.wiley.com). DOI: 10.1002/prot.20995

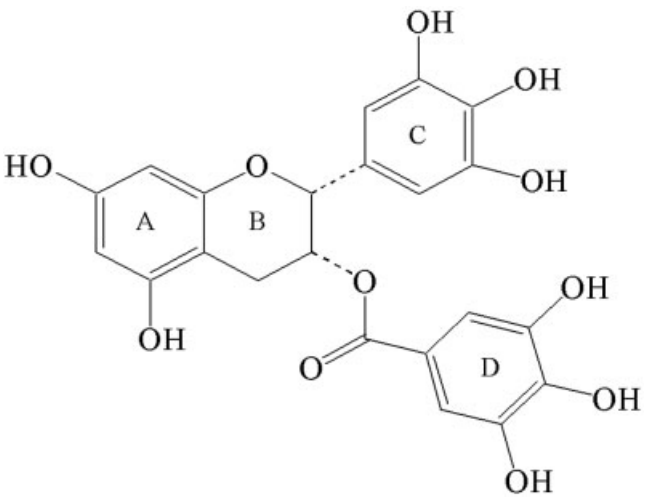

Fig. 1. Chemical structure of EGCG.

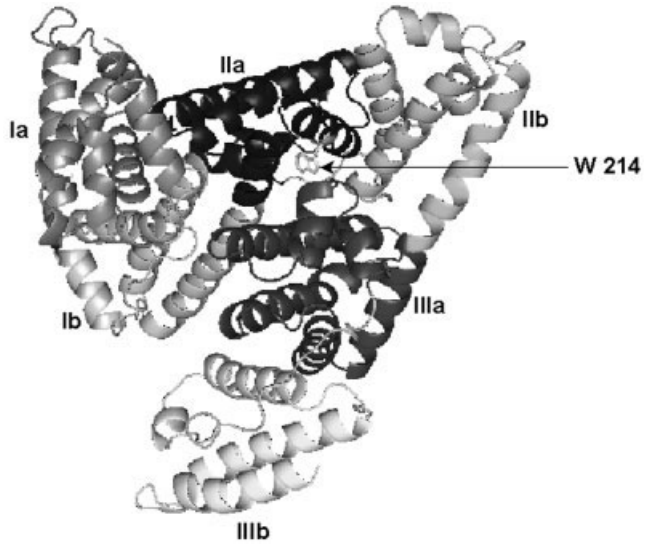

Fig. 2. Cartoon representation of HSA (PDB entry 1AO6). Each subdomain has been marked and the location of Trp 214 shown.

the mode of interactions of these compounds with their respective target proteins at the molecular level. Several recent studies have demonstrated that flavonoids, such as quercetin and rutin, isoflavone genistein, are carried in human blood by serum albumin (HSA) in the form of complexes between albumin and quercetin 3-O conjugates.[16–21] A recent investigation showed that quercetin oxidized by a peroxidase/hydrogen peroxide system bound covalently to certain proteins with high affinity for HSA.[22]

A recent report indicated that dietary flavonoids can be detected in plasma as serum albumin conjugates and this binding is believed to modulate the bioavailability of the flavonoids.[20] It is thus pertinent to consider the specific binding of these compounds to HSA. We have considered the binding of one such component, EGCG, which is a major component of green tea to HSA for a further understanding of how these compounds may be efficiently exploited to combat disease. A recent article in this journal highlighted the inhibition of chymotrypsin activity by the 20S proteasome by EGCG and a few other analogs. Docking studies were also used to assist in the understanding of the binding and inhibition of the protein to aid in further model development.[23]

The growing interest in green tea and its components thus provides a compelling reason to investigate the interaction of its major component, EGCG with HSA. In this study, we have explored the interaction of EGCG with HSA by biophysical methods, mainly fluorescence, FTIR, and CD studies. Thermodynamic parameters have been calculated according to the van't Hoff equation to determine the types of interactions involved. To substantiate our experimental studies, we have performed docking studies to obtain a clearer insight into the residues involved in the interaction.

MATERIALS AND METHODS

Materials

HSA (fatty acid free) fraction V and EGCG were from Sigma. D_2O was from Acros Organics and all other reagents were from SRL India. All solutions were prepared in 20 mM phosphate buffer of pH 7.0. The concentrations of HSA and EGCG were determined spectrophotometrically (PerkinElmer UV-Vis spectrophotometer model Lambda 25) using ϵ_{280} (HSA) = 35,500 M^{-1} cm^{-1} [24] and ϵ_{270} (EGCG) = 11,920 M^{-1} cm^{-1}.[25]

Fluorescence Spectroscopy

Fluorescence spectra were recorded on a Hitachi-850 spectrofluorometer (Japan) in a 1-cm quartz cell using an excitation wavelength of 295 nm. The excitation and emission bandwidths were 5 nm. The emission spectra were recorded from 310 to 400 nm. A quantitative analysis of the interaction between EGCG and HSA was performed by fluorimetric titration. HSA solution, 2.4 mL of 2.14×10^{-6} M, was titrated by successive addition of EGCG solution to reach a final concentration of 5.17×10^{-5} M in EGCG.

The binding parameters for the HSA–EGCG complex have been calculated at 293, 303, 308, and 313 K from fluorescence quenching data using the procedure of Scatchard.[26] This method is based on the general equation:

$$\frac{r}{D_f} = nK - rK \tag{1}$$

where r is the moles of EGCG bound per mole of protein, D_f is the molar concentration of free EGCG, n is the binding stoichiometry per class of binding sites, and K is the equilibrium binding constant.

Fluorescence quenching was also analyzed using the modified Stern-Volmer equation[27]:

$$\frac{F_0}{\Delta F} = \frac{1}{f_a K_a [Q]} + \frac{1}{f_a} \tag{2}$$

where $\Delta F = F_0 - F$; F_0 and F are the relative fluorescence intensities in absence and presence of the quencher, respectively, f_a is the fraction of fluorophore accessible to

the quencher, [Q] is the concentration of quencher, and K_a is the Stern-Volmer quenching constant. The plots of $F_0/\Delta F$ versus $1/[Q]$ yield $1/f_a$ as the intercept, and $1/(f_aK_a)$ as the slope. From the intercept and slope we calculate the K_a and f_a values.

Considering that the enthalpy change ($\Delta H°$) does not vary significantly over this temperature range, then its value and that of $\Delta S°$ can be calculated using the van't Hoff equation:

$$\ln K = -\frac{\Delta H°}{RT} + \frac{\Delta S°}{R} \quad (3)$$

where K is the binding constant at the corresponding temperature and R is the gas constant. The plot of $\ln K$ against I/T is a straight line, the equation of which provides the enthalpy ($\Delta H°$) and entropy ($\Delta S°$) changes on binding. The free energy of binding is estimated from the following relationship:

$$\Delta G° = \Delta H° - T\Delta S° \quad (4)$$

FTIR Spectroscopic Measurements

HSA, 17.5 mg/mL, was dissolved in 20 mM phosphate buffer of pD 7.2 in 99.9% D_2O giving a concentration of 0.263 mM. Three sets of HSA–EGCG solutions were prepared maintaining final ligand concentrations of 4.6, 46, and 460 μM, respectively. FTIR measurements were conducted at 25°C on a Nexus-870 FTIR spectrometer (Thermo Nicolet Corporation). Twenty-five microliters of sample solution was placed between a pair of CaF_2 discs (32-mm diameter). The sample holder assembly was placed on a mount inside the sample compartment of the FTIR instrument. The instrument was continuously purged with dry air and after sample insertion purging was continued for at least 2 min before any data collection. For each spectrum, a 256-scan interferogram was collected in a single beam mode with 4 cm^{-1} resolution. Control buffer spectra were recorded under identical conditions and the background was collected before every sample.

IR Spectra Processing Procedure

The secondary structure content of HSA and the HSA complex with EGCG was determined following the method of Byler and Susi.[28] The spectra obtained after buffer subtraction were smoothed by an 11-point Savitsky-Golay smooth function to reduce the noise. The protein secondary structure was determined from the amide I band located between 1,700 and 1,600 cm^{-1}. Fourier self-deconvolution and secondary derivative calculations were applied to estimate the number and position of the component bands. Based on these parameters, a multiple Gaussian curve-fitting process was performed in the region 1,700–1,600 cm^{-1} of the amide I band to quantify the area of each component. The relative percentage of the secondary structural elements was obtained from the area under the Gaussian curve.[28–31]

CD Measurements

CD measurements were made on a Jasco-810 automatic recording spectrophotometer, using a 2-mm path length at 25°C. The spectra were recorded in the range of 190–240 nm with a scan rate of 30 nm/min and a response time of 4 s. Three scans were accumulated for each spectrum. For CD studies, the concentration of HSA was 1.5×10^{-6} M, the HSA/EGCG ratios in complexes were 1:1.5 and 1:3. Results were expressed as $\Delta\epsilon$ and the secondary structure was determined using DICHROWEB,[32] an online server for protein secondary structure analyses from CD spectroscopic data.

Docking Studies

The crystal structure of HSA (PDB entry 1AO6) was downloaded from the PDB.[33] The three-dimensional structure of EGCG was generated by Sybyl 6.92 (Tripos Inc., St. Louis, MO) and the energy minimized conformation was obtained with the help of the TRIPOS force field using Gasteiger-Hückel charges with a gradient of 0.005 kcal/mole. The other parameters, dielectric constant, iteration number, maximum displacement, minimum energy change, simplex threshold, and simplex iteration, were set to 1.0, 1,000, 0.01, 0.05, 1,000, and 20, respectively. FlexX single molecule docking software was used for the docking of EGCG to HSA. The ranking of the generated solutions is performed using a scoring function as mentioned by Rarey et al.[34] which estimates the free binding energy ΔG of the protein–ligand complex. PyMol[35] was used for visualization and measurement of distances between the ligand and the receptor.

The ASA of HSA (uncomplexed) and the HSA–EGCG docked complex were calculated using NACCESS.[36] The EGCG structure corresponding to the highest rank as obtained from FlexX docking was chosen and composite coordinates were generated to form the docked complex. If a residue lost more than 5 $Å^2$ ASA when going from the noncomplexed to the complexed state, it was considered as being involved in the interaction.

RESULTS AND DISCUSSION

Analysis of Fluorescence Quenching of HSA

The fluorescence spectra of HSA in the absence and presence of EGCG in 20 mM phosphate buffer of pH 7.0 were measured with an excitation wavelength of 295 nm. HSA shows a strong fluorescence emission with a peak at 343 nm on excitation at 295 nm because of its single tryptophan residue (Trp 214). EGCG was nonfluorescent under these experimental conditions. The fluorescence intensity of HSA gradually decreased on addition of EGCG, indicating that EGCG interacts with the HSA. One representative fluorescence titration spectra at 20°C is shown in Figure 3. We observed a red shift of the wavelength maxima of HSA from 343 to 355 nm on addition of EGCG. This is indicative of a shift to a more polar environment.

The association constants K and binding stoichiometry n for the HSA–EGCG complex at 293, 303, 308, and 313 K were calculated from a Scatchard plot (Fig. 4). From the modified Stern-Volmer plot shown in Figure 5, the fractional accessibility of Trp 214 that is accessible to the quencher can be calculated. This was found to be 0.68, 0.74, 0.72, and 0.83 for 293, 303, 308, and 313 K, respec-

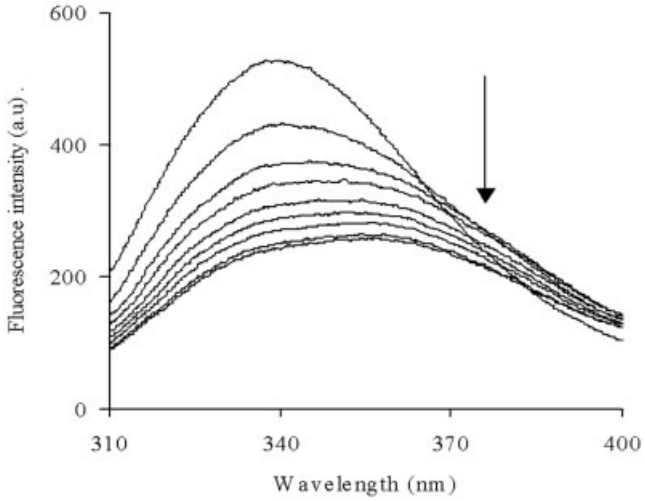

Fig. 3. Fluorescence spectra of the HSA–EGCG system. The concentration of HSA was 2.13×10^{-6} M and EGCG concentration increased from 0 to 5.17×10^{-5} M. T = 293 K; pH 7.0; λ_{ex} = 295 nm.

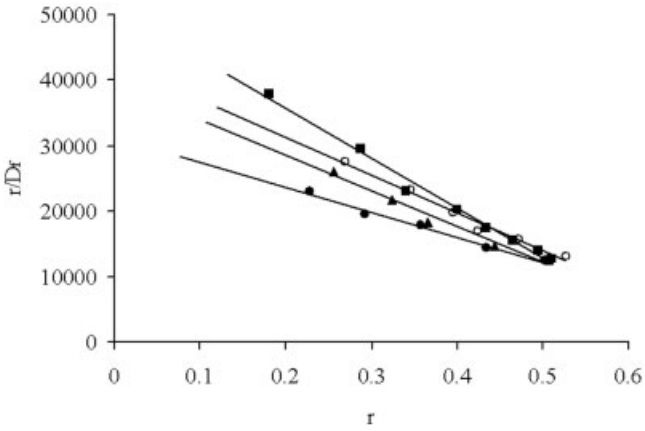

Fig. 4. Scatchard plot for the HSA–EGCG system at pH 7.0. HSA concentration: 2.13×10^{-6} M; ■, 293 K; ○, 303 K; ▲, 308 K; ●, 296 K; λ_{ex} 295 nm.

tively. The observed increase in fractional accessibility with increasing temperature may be attributed to slight structural changes in subdomains IIa making the Trp 214 more accessible. The binding parameters at four different temperatures for HSA–EGCG interaction were calculated from the Stern-Volmer plot. The quenching constant K_a was calculated as 6.85×10^4, 5.48×10^4, 5.34×10^4, and 3.66×10^4 M at 293, 303, 308, and 313 K, respectively, with an average n value of 0.74. The binding parameters are shown in Table I. The linear Scatchard plots indicate that EGCG binds to a single class of sites on HSA, which is in agreement with the number of binding sites n (Table I). From the Scatchard equation, the binding constants K for the reaction at 293, 303, 308, and 313 K were calculated and the values are 7.63×10^4, 5.78×10^4, 5.48×10^4, and 3.83×10^4 M, respectively. It was also found that binding constants decrease with increase in temperature suggesting that the temperature has a pronounced effect on HSA–EGCG binding.

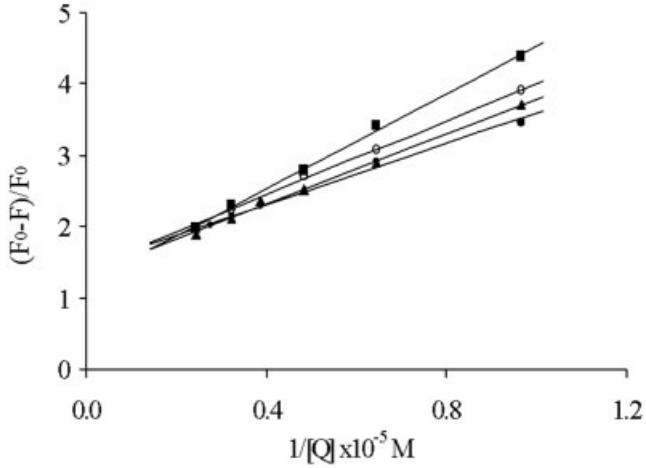

Fig. 5. Modified Stern-Volmer plots of the HSA–EGCG system: HSA concentration: 2.13×10^{-6} M; pH 7.0; ■, 293 K; ○, 303 K; ▲, 308 K; ●, 296 K; λ_{ex} 295 nm.

CD Studies

CD spectra of HSA exhibit two negative bands in the ultraviolet region at 209 and 221 nm as shown in Figure 6. This is characteristic of the α-helical structure of a protein. The secondary structure was determined using CDSSTR method in DICHROWEB, an online server for protein secondary structure analysis. By this method, it was found that the α-helical content of the protein changed from 57 to 54% upon binding with EGCG. There is a slight increase in the β-sheet and unordered structure of the protein. From the above CD analysis, it is evident that interaction of EGCG with HSA causes a slight conformational change of the protein, leading to a loss in its helical content.

FTIR Studies

Hydrogen bonding and the coupling between transition dipoles are the key factors that have a crucial role in governing the conformational sensitivity of the amide bands in the protein. The protein amide I band at 1,650–1,654 cm^{-1} (mainly attributable to C═O stretching) and amide II band at 1,548–1,560 cm^{-1} (C—N stretch coupled with N—H bending mode) are related to the secondary structure of proteins.[29,30] The difference spectra also provide information about the conformational changes that arise because of complex formation.[37] The changes observed in the FTIR spectra are attributable to the interaction of the amide I and amide II bands of HSA with EGCG. Figure 7(a) represents the FTIR spectra before and after binding of EGCG to HSA for varying concentrations of EGCG. The amide I peak position shifts from 1,650 cm^{-1} (free HSA) to 1,647 cm^{-1} (HSA–EGCG complex). This implies that the secondary structure of the protein is affected on complex formation. A quantitative analysis of this change is presented later. In the amide II region, apart from the peak at 1,567 cm^{-1} (free HSA) that essentially remains unaltered on complex formation, two new peaks are generated at 1,549 and 1,517 cm^{-1}, respectively, because of

TABLE I. Thermodynamic Parameters for EGCG Binding to HSA

Temperature (K)	K_a (10^4) (Stern-Volmer)	K (10^4) (Scatchard method)	n	$\Delta G°$ (kJ/mol)	$\Delta H°$ (kJ/mol)	$\Delta S°$ J/mole/K
293	6.85	7.63	0.67	−27.22		
303	5.48	5.78	0.74	−27.42	−22.59	16.23
308	5.34	5.48	0.72	−27.53		
313	3.66	3.83	0.81	−27.63		

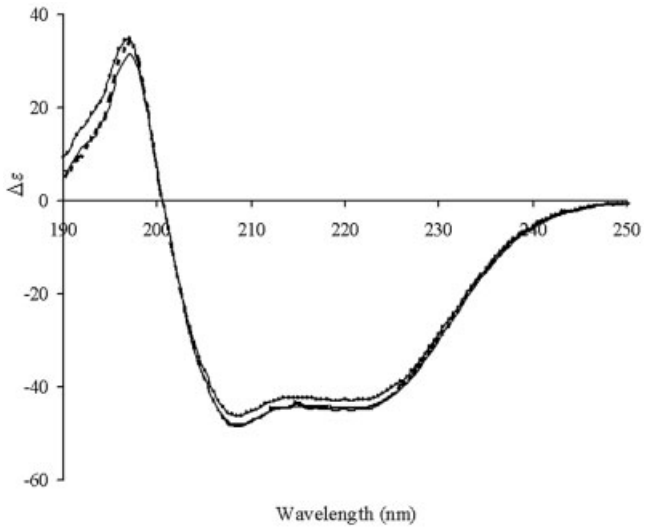

Fig. 6. CD spectra of HSA–EGCG complexes at pH 7.0. HSA (1.5 μM) (——); 1:1.5 HSA and EGCG (—); 1:3 HSA and EGCG (- · · · -).

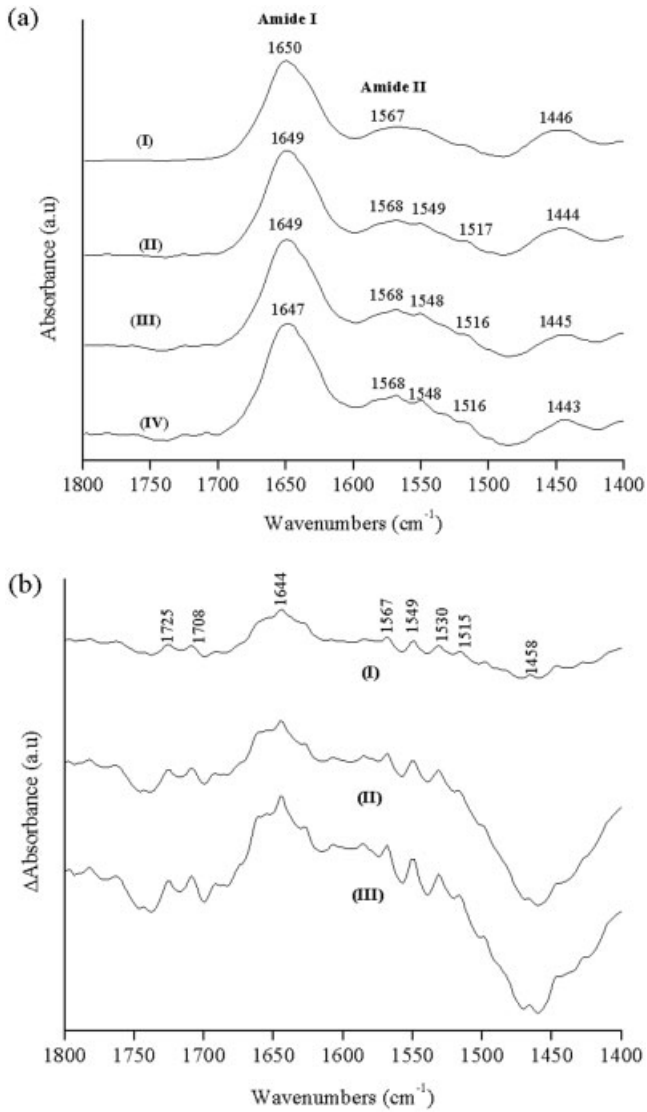

Fig. 7. **a:** FTIR spectra of HSA only (I) and HSA bound to EGCG (II–IV). **b:** FTIR difference spectra [(HSA solution + EGCG solution) − (HSA solution)] with HSA bound to EGCG (I–III). Concentration ratios 1:0.0175; 1:0.175; 1:1.75, respectively.

the interaction with EGCG. The peak at 1,517 cm^{-1} is probably attributable to Tyr 452 of helix 4 of subdomain IIIa because Tyr residues are associated with a sharp band at 1,515 cm^{-1}.[30,31] The involvement of Tyr 452 is also observed in the docked structure and is found to lose ~13 $Å^2$ of its ASA on complex formation. The shift observed in the peak at 1,446 cm^{-1} arises because of (i) CH_2 and CH_3 bending modes of the side-chains and (ii) bending modes of traces of HOD.[30,31] Bands appearing near 1,446 cm^{-1}, however, are not involved in the secondary structure calculations of either the protein or the protein–EGCG complex.

The difference spectra of the interaction of HSA with three different concentrations of EGCG are given in Figure 7(b). At low EGCG concentration (4.6 μM), positive peaks appear at 1,644 cm^{-1} (amide I) and 1,567, 1,549, 1,530 cm^{-1} (amide II). The presence of the weak positive derivative feature around 1,515 cm^{-1} may be attributed to the Tyr vibration.[30,31] The presence of the negative feature at 1,458 cm^{-1} is attributed to the loss of intensity of the CH_2 and CH_3 bending modes of the side-chains. As the concentration of EGCG is increased 10-fold to 46 μM [Fig. 7(b) (II)] and 100-fold [Fig. 7(b) (III)], the intensity of each peak gradually enhances without changes in the peak positions.

To further understand the details of the interaction, a quantitative analysis of the protein secondary structure for free HSA and its EGCG complexes in D_2O was undertaken. The results are given in Figure 8. The free protein contained 61% α-helix, 29% β-sheet, 10% turn. Because of the interaction of EGCG with HSA, the α-helix content was reduced from 61 to 49%. A reduction in the α-helical content was also obtained from CD studies as discussed earlier. The β-sheet and turn content increased from 29 to 39% and 10 to 12%, respectively, at higher concentrations of EGCG (Table II).

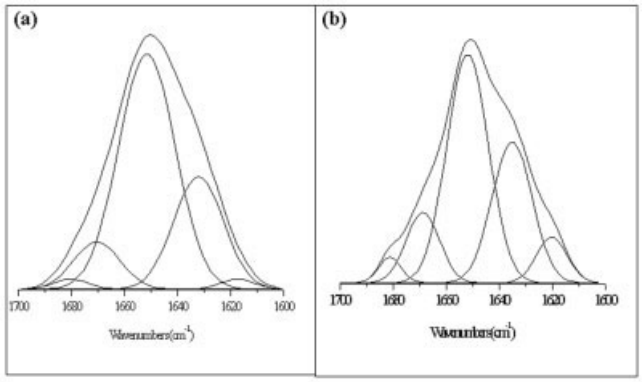

Fig. 8. Curve-fitted amide I (1,700–1,600cm^{-1}) region of (**a**) free HSA and (**b**) HSA–EGCG complex in 20 mM phosphate of pD 7.2 buffer solution.

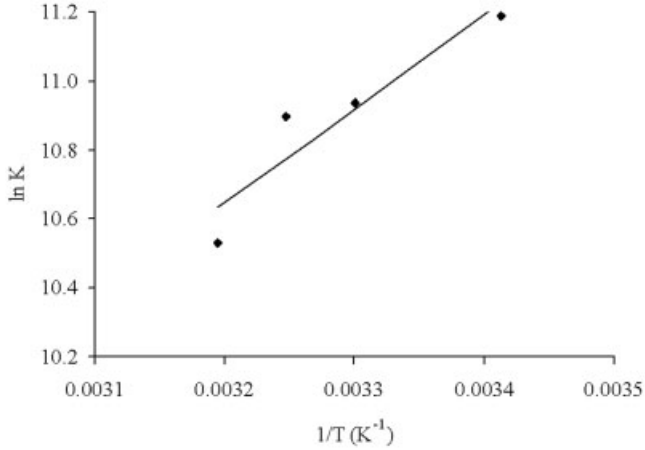

Fig. 9. Temperature dependence of binding constant (van't Hoff plot) at pH 7.0; HSA concentration: 2.13 × 10^{-6} M.

TABLE II. Secondary Structure Determination for Free HSA and HSA–EGCG Complex in D_2O Buffer of pH 7.2

Secondary structural elements	Peak position (cm^{-1})	HSA (%)	HSA–EGCG complex (%)
β-Sheet	1,617–1,635	27	36
α-Helix	1,652	61	49
β-Anti	1,680–1,682	2	3
Turn	1,668–1,670	10	12

Mode of Binding

Thermodynamic parameters

Hydrogen bonds, van der Waals, hydrophobic, and electrostatic interactions are the major interactions that have a key role in protein-ligand binding.[35,36] The thermodynamic parameters, free energy ($\Delta G°$), enthalpy ($\Delta H°$), and entropy ($\Delta S°$) of interaction provide an insight into the binding mode. For this purpose, the temperature dependence of the binding constants was studied. Experiments were conducted at 293, 303, 308, and 313 K because HSA does not undergo any gross structural change in this temperature range. From the temperature dependence of the binding constant, it is possible to calculate the thermodynamic functions involved in the binding process. The binding parameters of the HSA–EGCG complex at the four temperatures were estimated from a van't Hoff plot (Fig. 9). The mean K values obtained from the Stern-Volmer equation and the Scatchard plot were used to plot the data according to Eq. (3) in Materials and Methods. A least-square regression line fitted to the data gave an R^2 value of 0.87. The $\Delta H°$ and $\Delta S°$ values were obtained from the slope and intercept, respectively.

From Table I it is observed that the formation of the HSA–EGCG complex is accompanied by a negative enthalpy change ($\Delta H° = -22.59$ kJ/mol) and a positive entropy change ($\Delta S° = 16.23$ J/mole/K), which indicates that the binding process is enthalpy driven. The negative sign for $\Delta G°$ (-27.45 ± 0.17 kJ/mol) indicates the spontaneity of binding of EGCG to HSA. The net $\Delta G°$ for the complete association process is essentially determined by the relative magnitude of positive $\Delta S°$ and negative $\Delta H°$.[38,39] For the HSA–EGCG system, the main source of the $\Delta G°$ value is derived from a substantial contribution from the $\Delta H°$ factor. The partial immobilization of the protein and the ligand occurs in an initial step involving hydrophobic association[39] that results in a positive $\Delta S°$. In the subsequent interacting complex, the negative $\Delta H°$ contribution to the overall $\Delta G°$ may be associated with van der Waals interactions and hydrogen bonding.

Docking studies

The experimental results obtained from fluorescence, CD, and FTIR studies were substantiated by docking experiments in which EGCG was docked to HSA to determine the preferred binding site on the protein. The stereo-view docking pose of EGCG with HSA is shown in Figure 10. The docking shows that EGCG is located within the binding pocket of subdomain IIa and IIIa. The inside wall of the pocket is lined by hydrophobic side-chains whereas the entrance to the pocket is surrounded by positively charged residues such as Lys 195, Lys 199, Arg 218, Arg 222, His 242, and Arg 257. Trp 214 is part of helix 2 of subdomain IIa (represented as IIa-h2) that spans residues 208–223. We find that in the best docked conformation obtained, the hydroxy groups of ring C and D of EGCG are within hydrogen bonding distance of (i) Trp 214, Arg 218, and Gln 221 residues of IIa-h2; (ii) Asn 295 that resides in the loop in between IIa-h6 and IIb-h1; and (iii) Asp 451 of IIIa-h4. Docking of EGCG creates a hydrophilic environment near Trp 214. This may be the reason for the large red shift observed in the fluorescence spectra on binding of EGCG.

To further identify the residues taking part in the interaction, we calculated the ASA for HSA and the HSA–EGCG complex. Residues in which the absolute ASAs have decreased by more than 5 Å^2 on complex formation are given in Table III. We find that most of the residues involved in the interaction belong to subdomains IIa and IIIa as expected from our experimental results. The inside pocket of subdomain IIa which comprises site I is predominantly hydrophobic in nature with the entrance surrounded by positively charged residues. Between these

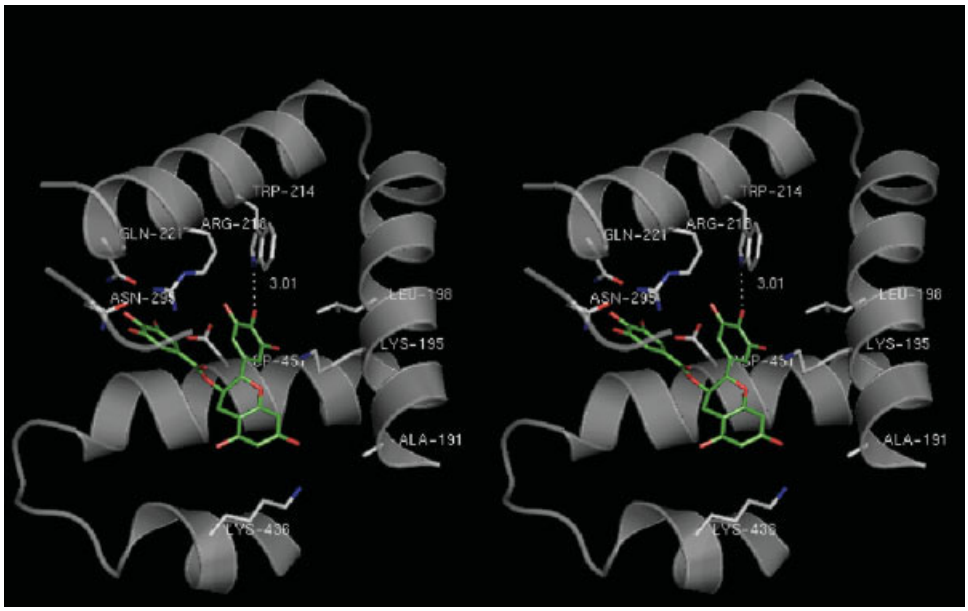

Fig. 10. Stereoview docking pose of HSA and EGCG. Residues of interest and EGCG have been represented as sticks. The protein chain has been truncated at different points for clarity. The binding pocket of site I is clearly visible with Trp 214 within hydrogen bonding distance of EGCG. The entrance to the pocket is lined with polar residues.

TABLE III. The ASA of HSA (Uncomplexed) and the HSA–EGCG Docked Complex

Residue	ASA in Å^2 (HSA)	ASA in Å^2 (HSA–EGCG)	ΔASA (Å^2)	Location
Ala 191	39.24	27.08	12.16	Ib-h4
Lys 195	91.36	47.10	44.26	Ib-h4
Leu 198	28.99	21.99	7.00	IIa-h1
Trp 214	61.74	40.31	21.43	IIa-h2
Arg 218	41.96	04.96	37.00	IIa-h2
Glu 292	92.68	85.39	7.29	IIa-h6
Asn 295	55.89	43.82	12.07	Loop in between IIa-h6 and IIb-h1
Lys 436	97.93	74.06	23.87	IIIa-h3
Pro 447	25.80	6.61	19.19	IIIa-h4
Cys 448	39.21	9.18	30.03	IIIa-h4
Asp 451	30.24	0.03	30.21	IIIa-h4
Tyr 452	36.91	24.13	12.78	IIIa-h4
Val 455	17.81	7.86	9.95	IIIa-h4

Lys 195 and Arg 218 lose the maximum surface area on binding (44 and 37 Å^2, respectively). These studies support our experimental observations.

CONCLUSION

In this article, the binding of EGCG to HSA under physiological conditions has been presented by fluorescence methods in combination with CD, FTIR, and docking studies. The results show that EGCG is a strong quencher of the fluorescence of HSA and binds to the protein with high affinity. The binding of EGCG to HSA increases the polar environment of the Trp residue resulting in a red shift in the fluorescence spectra. The binding parameters calculated from Stern-Volmer plots and Scatchard plots at varying temperatures are in agreement with each other. CD and FTIR studies indicate that there is an alteration in the protein secondary structure because of the interaction of HSA with EGCG. There is a distinct loss in α-helical content on ligand binding. The thermodynamic parameters indicate that after a possible initial hydrophobic association, contributions from van der Waals interactions and hydrogen bonding are primarily responsible for the overall negative ΔG°. The interaction has also been investigated by docking studies. In the docked conformation, it has been observed that EGCG is within hydrogen bonding distance of Trp 214. The ASA calculations also substantiate the above observations, where residues at the entrance to site I, Lys 195 and Arg 218 lose their solvent accessibility because of binding.

ACKNOWLEDGMENTS

Financial support from the Department of Science and Technology (DST) and Ministry of Human Resource Devel-

opment (MHRD), Government of India, is acknowledged. We are grateful to Bose Institute, Kolkata and Central Research Facility, IIT Kharagpur for experimental studies. T.K.M. thanks CSIR, New Delhi for a fellowship.

REFERENCES

1. Cutter H, Wu LY, Kim C, Morre DJ, Morre DM. Is the cancer protective effect correlated with growth inhibitions by green tea (−)-epigallocatechin gallate mediated through an antioxidant mechanism? Cancer Lett 2001;162:149–154.
2. Pietta PG. Flavonoids as antioxidants. J Nat Prod 2000;63:1035–1042.
3. Balentine DA. Manufacturing and chemistry of tea. In: Ho C-T, Huang M-T, Lee CY, editors. Phenolic compounds in food and their effects on health, analysis, occurrence, and chemistry. Washington, DC: American Chemical Society; 1992. p 102–117.
4. Tosetti F, Ferrari N, De Flora S, Albini A. Angioprevention: angiogenesis is a common and key target for cancer chemopreventive agents. FASEB J 2002;16:2–14.
5. Lambert JD, Yang CS. Cancer chemopreventive activity and bioavailability of tea and tea polyphenols. Mutat Res 2003;523:201–208.
6. Fujiki H, Suganuma M, Imai K, Nakachi K. Green tea: cancer preventive beverage and/or drug [mini-review]. Cancer Lett 2002; 188:9–13.
7. Cao Y, Cao R. Angiogenesis inhibited by drinking tea. Nature 1999;398:381.
8. Zhong Z, Connor HD, Froh M, et al. Polyphenols from *Camellia sinenesis* prevent primary graft failure after transplantation of ethanol-induced fatty livers from rats. Free Radic Biol Med 2004;36:1248–1258.
9. Narumi S, Mikae O, Masahiro I, Koji F. Differences in antioxidative efficiency of catechins in various metal-induced lipid peroxidations in cultured hepatocytes. J Health Sci 2001;47:99–106.
10. Brown JE, Khodr H, Hider RC, Rice-Evans CA. Structural dependence of flavonoid interactions with Cu^{2+} ions: implications for their antioxidant properties. Biochem J 1998;330:1173–1178.
11. Kragh-Hansen U. Molecular aspects of ligand binding to serum albumin. Pharmacol Rev 1981;33:17–53.
12. Muller WE, Wollert U. Human serum albumin as a 'silent receptor' for drugs and endogenous substances. Pharmacology 1979;19:56–59.
13. He XM, Carter DC. Atomic structure and chemistry of human serum albumin. Nature 1992;358:209–215.
14. Sugio S, Kashima A, Mochizuki S, Noda M, Kobayashi K. Crystal structure of human serum albumin at 2.5 Å resolution. Protein Eng 1999;12:439–446.
15. Lamson SW, Brignall MS. Antioxidants and cancer. Part 3. Quercetin. Altern Med Rev 2000;5:196–208.
16. Sengupta B, Sengupta PK. The interaction of quercetin with human serum albumin: a fluorescence spectroscopic study. Biochem Biophys Res Commun 2002;299:400–403.
17. Zsila F, Bikádi Z, Simonyi M. Probing the binding of the flavonoid, quercetin to human serum albumin by circular dichroism, electronic absorption spectroscopy and molecular modelling methods. Biochem Pharmacol 2003;65:447–456.
18. Boulton DW, Walle UK, Walle T. Extensive binding of the bioflavonoid quercetin to human plasma proteins. J Pharm Pharmacol 1998;50:243–249.
19. Dangles O, Dufour C, Manach C, Morand C, Remesy C. Binding of flavonoids to plasma proteins. Methods Enzymol 2001;335:319–333.
20. Dufour C, Dangles O. Flavonoid–serum albumin complexation: determination of binding constants and binding sites by fluorescence spectroscopy. Biochim Biophys Acta 2005;1721:164–173.
21. Manach C, Morand C, Crespy V, et al. Quercetin is recovered in human plasma as conjugated derivatives which retain antioxidant properties. FEBS Lett 1998;426:331–336.
22. Kaldas MI, Walle UK, van der Woude H, McMillan JM, Walle T. Covalent binding of the flavonoid quercetin to human serum albumin. J Agric Food Chem 2005;53:4194–4197.
23. Smith DM, Daniel KG, Wang Z, Guida WC, Chan T-H, Dou PQ. Docking studies and model development of tea polyphenol proteasome inhibitors: applications to rational drug design. Proteins 2004;54:58–70.
24. Gonzalez-Jimenez J, Frutos G, Cayre I, Cortijo M. Chlophenir amine binding to human serum albumin by fluorescence quenching measurements. Biochimie 1991;73:551–556.
25. Pelillo M, Cuvelier ME, Biguzzi B, Toschi TG, Berset C, Lercker G. Calculation of the molar absorptivity of polyphenols by using liquid chromatography with diode array detection: the case of carnosic acid. J Chromatogr A 2004;1023:225–229.
26. Scatchard G. The attractions of proteins for small molecules and ions. Ann NY Acad Sci 1949;51:660–673.
27. Lakowicz JR. Principles of fluorescence spectroscopy. New York: Plenum Press; 1991.
28. Byler D, Susi H. Examination of the secondary structure of proteins by deconvolved FT-IR spectra. Biopolymers 1986;25:469–487.
29. Dong AC, Huang P, Caughey WS. Protein secondary structures in water from second-derivative amide I infrared spectra. Biochemistry 1990;29:3303–3308.
30. Susi H, Byler DM. Protein structure by Fourier transform infrared spectroscopy: second derivative spectra. Biochem Biophys Res Commun 1983;115:391–397.
31. Susi H, Byler DM. Resolution-enhanced Fourier transform infrared spectroscopy of enzymes. Methods Enzymol 1986;130:290–311.
32. Whitmore L, Wallace BA. DICHROWEB: an online server for protein secondary structure analyses from circular dichroism spectroscopic data. Nucleic Acids Res 2004;32:W668–W673.
33. Berman M, Westbrook J, Feng Z, et al. The Protein Data Bank. Nucleic Acids Res 2000;28:235–242.
34. Rarey M, Kramer B, Lengauer T, Klebe G. A fast flexible docking method using an incremental construction algorithm. J Mol Biol 1996;261:470–489.
35. DeLano WL. The PyMOL molecular graphics system. San Carlos, CA: DeLano Scientific; 2004. http://www.pymol.sourceforge.net.
36. Hubbard SJ, Thornton JM. 'NACCESS.' Computer Program, Department of Biochemistry and Molecular Biology, University College London; 1993.
37. Neault JF, Tajmir-Riahi HA. Interaction of cisplatin with human serum albumin. Drug binding mode and protein secondary structure. Biochim Biophys Acta 1998;1384:153–159.
38. Timaseff SN. Thermodynamics of protein interactions. In: Peeters H, editor. Proteins of biological fluids. Oxford: Pergamon Press; 1972. p 511–519.
39. Ross PD, Subramanian S. Thermodynamics of protein association reactions: forces contributing to stability. Biochemistry 1981;20: 3096–3102.